A. Ben Meriem, S. Bouguecha, S. Elsayed Aly / International Journal of Engineering Research and Applications (IJERA) ISSN: 2248-9622 www.ijera.com
Vol. 3, Issue 1, January -February 2013, pp.354-368

Solar-Driven Integrated Ro/Nf For Water Desalination

A. Ben Meriem[a], S. Bouguecha[b], S. Elsayed Aly[b]

[a] LETM/ CERTE, BP 95 Hammam-Lif 2050, Tunisia

[b] Department of Thermal Engineering and Desalination Technology, Faculty of Engineer, King Abdul-Aziz University, P.B: 80204 Jeddah 21589, Fax: 6401686, Tel: 6402000, Kingdom of Saudi Arabia.

Abstract

This article presents an experimental study where two different modules are integrated, i.e. a reverse osmosis (RO) module, and a nano-filtration (NF) module, for brackish water desalination unit. Photovoltaic (PV) panels power the setup. The performance for each of the modules was evaluated separately. Then both modules were integrated together, either in series or in parallel. The performance of the integrated setup is investigated using various feed solutions. Separately, the RO module exhibits higher retention (RT) for divalent ions, than that for the mono valence ions. The retention of the RO was higher than that for the NF. The NF module exhibits higher flux and lower specific energy consumption (SEC) than that of the RO module. Results of the integrated arrangement showed that, for a given feed solution, the series arrangement, would offer an opportunity to operate the desalination unit at higher recovery ratio (RR), and low SEC. The parallel arrangement, presents a reasonable solution for desalinating saline brackish water, with a lower risk of scale formation on the RO membrane.

Keywords: Reverse Osmosis, Nano-filtration, Solar Energy, Desalination, Brackish water

1. Introduction

During last decades, many regions around the world, suffered from severe fresh water shortages. Satisfying the increasing demand for fresh water depends on the advancement achieved in the water desalination technologies as a reliable source of freshwater. Desalination market has greatly expanded in recent decades and it is expected to continue expanding in the coming decades too, particularly in the Mediterranean, Middle East and North Africa regions [1].

Currently, reverse osmosis (RO) leads thermal desalination in terms of market share [2]. The performance of such a pressure-driven process depends on the properties of a semi-permeable membrane used to separate freshwater produced (permeate) from the saline feed. The current RO membranes can retain about 98–99.5% of the dissolved salts in the feed water with typical operating pressures ranging between 10 to 15 bars for brackish water and between 55 to 65 bars for seawater. The membrane fouling and scaling limits the recovery ratio (RR). Overall water RR can be as high as 90% for brackish water desalination systems [2-4].

The continuous depletion of fossil fuel raised the fuel price, which would impose high cost for the energy required to drive the RO's high-pressure pump. Indeed, using a renewable solar energy source, e.g. photovoltaic (PV), to provide the required energy for the membrane process, presents a promising alternative for using a fossil fuel. Employing the PV would improve the process sustainability, and reduce the operational costs of the desalination process.

A large number of solar-powered RO desalination experimental units have been built and tested in countries with high solar radiation. Alawaji et al. [5] estimated that solar tracking with seasonal plate tilt angle variations could increase the yearly average permeate flow of a PV-RO desalination plant in Saudi Arabia by 13% percent. Abdullah et al. [6], using a PV-RO rig in Jordan, reported an increase of 15% of the permeate flow by using a one-axis automatic tracking system rather than a fixed tilt plate. Harrison et al. [7] demonstrated that, using solar tracking produced 60% more permeate flow than using a fixed array for a small unit with a capacity of 50 L/day. Integrating the PV in a RO plant, may involve using the feed water to cool the PV panels and thus preheating the feed water. The additional cost, for such integrated setup, could be as much as 10 % of the system capital cost. However, the PV electrical output could be improved by about 3%. Besides, the increase of the feed water temperature could produce 20 to 30 % extra water output from the RO process [8].

The development of energy recovery devices (ERD) for seawater desalination, are implemented in small-scale RO units. The use of ERD in seawater PV–RO desalination is rapidly becoming standard practice, e.g. Pelton turbines. Efficient devices for low flow rates are developed, such as Clark pumps, hydraulic motors, energy recovery pumps, and pressure exchangers. Studies comparing different recovery mechanisms applied to PV-RO systems were inconclusive. The results from such studies indicated that, the selection of an efficient ERD for a particular system is a system dependent parameter.

In brackish water desalination, only a limited number of studies employed ERD devices. That

is mainly due to the low pressure of the concentrated brine effluent, besides, the high RR makes the expected energy recovery less critical [1]. Specific energy consumption (SEC) of about 2.0 kWh/m^3 is reported for a medium sized PV–RO plant with battery storage in Egypt, and plants with DC motors were developed and installed in the USA and Australia [9**].** Using conventional RO/PV combination, yields low recovery ratio, and high SEC [10].

Nano-filtration (NF) membranes are used for pretreatment of the feed in SWRO desalination plants. The NF membrane prevents fouling, scaling, and reduces the TDS of the feed water by 30-60% depending on the type of the NF membrane and the operating conditions [11-16].

Available literature on integrated RO, NF membranes, driven by PV panels, for water desalination is limited. In Australia, Andrea I. Schäfer et al. [17] tested a hybrid membrane system (Ultra filtration, NF, and RO) for brackish water desalination. The system was tested by applying different a pressures at the feed side, in order to investigate its effect on the permeate flux, RR, Retention (RT), and the SEC. The results showed that ultra filtration was effective in reducing the feed water high turbidity of up to 370 NTU. In addition, the flux and RR were increased by increasing the applied pressure, for the tested 1000 L/d unit. The RT for the multi valence ions was stable when it reaches 98% and above. The retention ratio for the mono valence ions varied between 88 and 95% depending on the applied pressure. The SEC for the tested unit with applied pressure of 7-15 bar, ranged from 3.0-5.5 and 2.0-3.1 kWh/m^3 for the BW30 and NF90 membranes, respectively.

Andrea Ghermandi et al. [18] discussed the advantages of using NF membranes for producing irrigation water, based on a simulated performance of a solar-assisted RO plant in the Arava Valley. They argued that the system would reduce the SEC by 40% compared with the RO plant, reduce the groundwater feed by 34%, and increase the total biomass production of the irrigated crops by 18%.

The present work is directed towards investigating the opportunities for brackish water desalination using an integrated RO/NF membranes setup, powered by PV panels for potable water production. The integrated system (RO / NF/PV) provides a substitute for the RO/PV conventional system. It is an experimental test setup for a pilot-scale desalination plant featuring RO, NF modules operating in series or parallel configurations, and powered by PV panels. The obtained results are discussed and compared with the performance for each of the RO, and the NF modules separately.

2- Experimental Procedure

The experimental set-up is designed, built, and tested in the laboratory. It is an integrated membrane desalination process, for brackish water desalination, employing both RO and NF modules. PV panels that generate electrical power for driving the high-pressure feed water pump power the setup.

2.1 Setup Description

The experimental setup used in the present work is shown in Fig. 1. The setup consists of:

1 - A feed pretreatment facility, where the feed water processed through an active carbon bed together with 5 micron cartridge filter. This is essential to protect the membrane modules from colloids, suspended matter and residual chlorine.

2 - A desalination facility consists of two modules; Reverse Osmosis (RO) module, model (AG2514TF/OSMONICS), Nano-Filtration (RO) module, model (HL2514TF/ OSMONICS), and a solar energy driven high-pressure pump mark BOOSTER. Both modules are spiral wound (polypropylene), able to handle waters with up to 2000 ppm (TDS).The RO module has an area 0.6 m^2, with a nominal capacity of 680 L/d for an applied pressure of 15 bar with a RT for NaCl from 99 % to 99.5 %. The area of the NF module is 0.6 m^2, with a nominal production of 830 L/d for an applied pressure of 6.9 bar and RT for MgSO4 of 98 %.

3 - Two photovoltaic (PV) panels (isofotón) assembled in series, with output DC current, 12 V each, and a maximum power output of 100 W. The PV panels are connected with electric power batteries having a 70-100 Ah capacity. The PV drives the high pressure feed pump; mark BOOSTER, connected to both of the RO and the NF modules. The pump is capable of supplying a feed rate of 189.27 L/d at a
maximum pressure 8 bar.

2.2 Monitoring and measurements

1 - The RR was controlled using the reject valve located downstream of both the RO and the NF modules.

2 - Pressure manometers indicate the flow conditions. The applied reduced pressure (ARP) is the ratio of the applied pressure to the maximum operating pressure of 7.5 bar and 6.5 bar for the RO and NF modules respectively.

3 - The flow is measured by means of a gradual bowl and chronometer.

4 - The electric conductivity for the flow (X in mS/cm) is measured by an interfacial sensor, the voltage and the current, are monitored by a regulator.

- The measure of the electric conductivity provides the flow salinity (C, NaCl g/L) according to the following relationship:

$$C = 2.75.10^{-3} X^2 + 5.20.10^{-1} X$$

- Different feed water solutions are used to characterize the RO and the NF modules, e.g.

a. Feed with a single solute of sodium chloride (NaCl) to provide solution with different concentrations, (C_1 = 3.37 g/L, C_2 = 3.94 g/L, and C_3 = 4.85 g/L).
b. Feed with multi-solutes {calcium sulfate ($CaSO_4$) and sodium chloride (NaCl)} at various mass fractions to provide solutions with $CaSO_4$ mass fraction of 20%, 50%, and 80%. The concentration total is 3.9 g/L.
c. Feed with a total salinity of 3.9 g/L {concentration potassium chloride (C_{KCl} = 26.6 mg/L), concentration of calcium sulfate (C_{CaSO4} = 581.5 mg/L), concentration of sodium chloride (C_{NaCl} = 1131.2 mg/L) and concentration of magnesium sulfate (C_{MgSO4} = 2161 mg/L)}, for the integrated setup.

5 - Feed water solutions were prepared using de-ionized water, and the chemical agents used are FLUKA type. The experiments were conducted at neutral pH (+7).

6 - The solutions of NaCl, KCl and $CaSO_4$ are analyzed, for calcium, potassium, magnesium and sodium by atomic absorption spectrometry (AAS) and for chloride by potentiometer Titrondo.

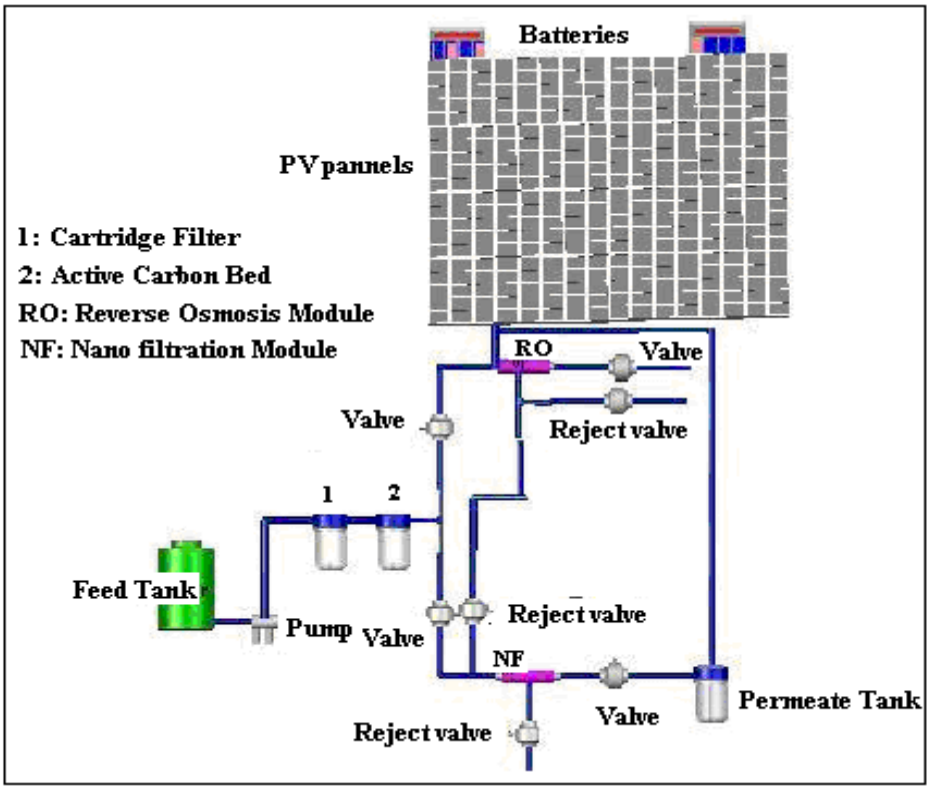

Figure 1: The experimental setup.

3. Results and Discussion

Experiments are conducted; first part of the tests is aimed to characterize each of the RO, NF modules separately. Second part of the tests is concerned with evaluating the performance of the integrated RO and NF modules.

3.1. Evaluation of the RO and NF modules, separately

3.1.1 - Single solute NaCl tests;

Figure 2 shows the performance of the RO and NF modules under an ARP of unity e.g. 7.5 bar and 6.5 bar for RO and NF modules respectively at different NaCl concentrations e.g. 3370 ppm, 3940 ppm, 4850 ppm. As for the NF module, the RT at low salt concentrations is higher than that at high concentrations. This is due to the linear relationship between the flux and the driving potential while the salt permeability is not linear with the concentration, the chemical potential difference that can be logarithmic related [19]. It is worth noticing that the flux for both modules decreases by increasing the NaCl concentration, though the RO flux is lower than that showed by the NF module.

The RT% of the NF module for the NaC1 decreases with increasing the salt concentration. This is typical for low-pressure RO and NF modules. That could be attributed to the Donnan effect due to the negatively charged NF membranes as reported by Rios et al. [20]. Here, the higher salt concentration will reduce the effective membrane charge and thus increases

consequently the co-ion ($C1^-$) concentration at the membrane. The rejection of the co-ion will be decreased due to the electro-neutrality, and the rejection of the counter ion will be reduced compared to that due to diffusion, within some limitations. The RT% is significantly higher for RO than that for NF. Colon et al. [21] have shown that the NF membrane has lower sodium chloride rejection than RO, but it has much higher water permeability. Both the RO and the NF modules have shown proportional increase of the SEC with the concentration increase. This is attributed to the reduction of driving potential due to the increase of osmotic pressure, which is related to the concentration. The SEC of the RO reached seven times than that of the NF module at ARP = 1.

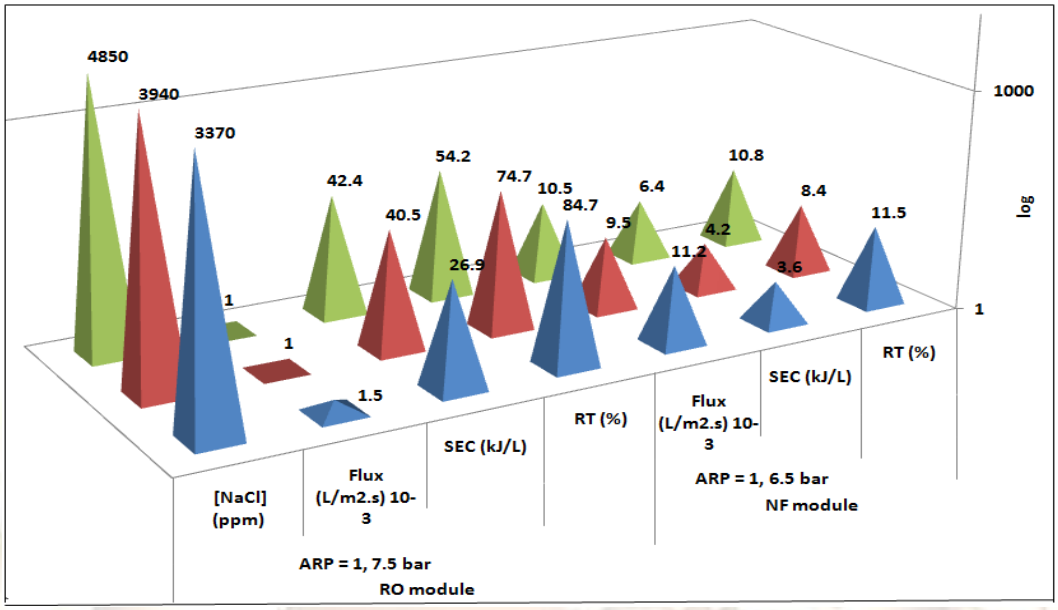

Figure 2: Characteristics for RO / NF module, using single salt

3.1.2 - Multi-solutes of $CaSO_4$ and NaCl tests

Figure 3 shows the results of RO and NF membranes at ARP = 1 and constant temperature of 20°C with multi-solutes solution. The flux for the RO and NF increases with increasing the fraction of $CaSO_4$ in the solution, and it is significantly higher for the NF compared to that for the RO. The RT% for RO is higher than that for the NF, which has a maximum of 94.27% and 66% for RO and NF respectively, realized at the highest fraction of $CaSO_4$ in the solution. The SEC increases with the $CaSO_4$ concentration in the solution. For the NF module, the SEC remains less than that for the RO module.

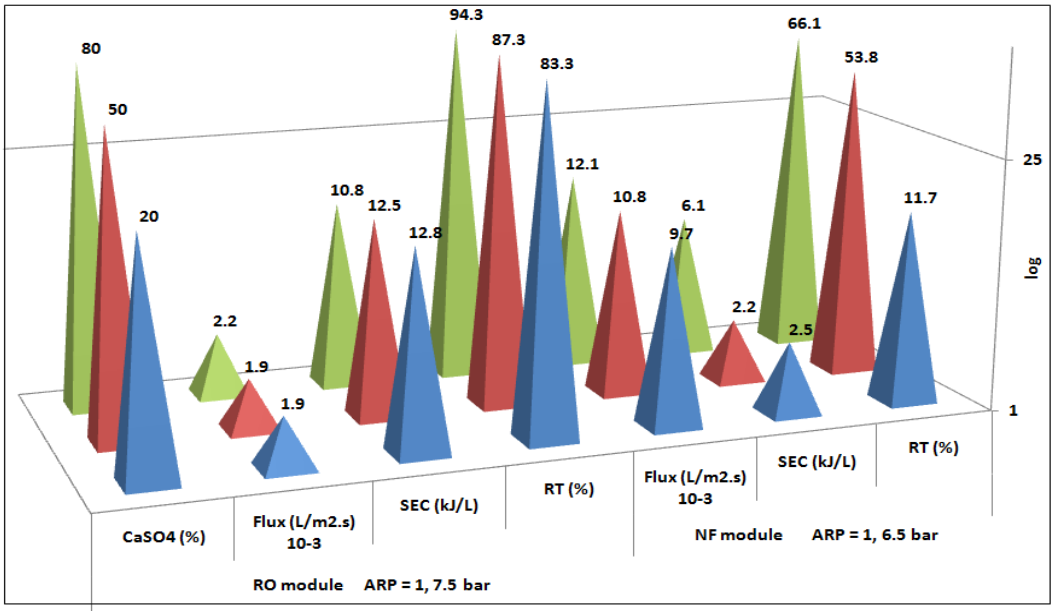

Figure 3: Characteristics for RO / NF module, using salt mixture.

3.1.3 - Selectivity evaluation for the RO and the NF membranes

The test results are given in Figs. 4 and 5 for the RT% in relation to the ARP. With 80% $CaSO_4$ in the solution, the figures show that the selectivity of both RO and NF membranes for the divalent ions (e.g.Ca^{2+}) is much higher than that for the mono valent ions (Na^+ and Cl^-). The RT % for the Ca^{2+} ions is 94 % and 91 %, for the RO and the NF modules respectively.

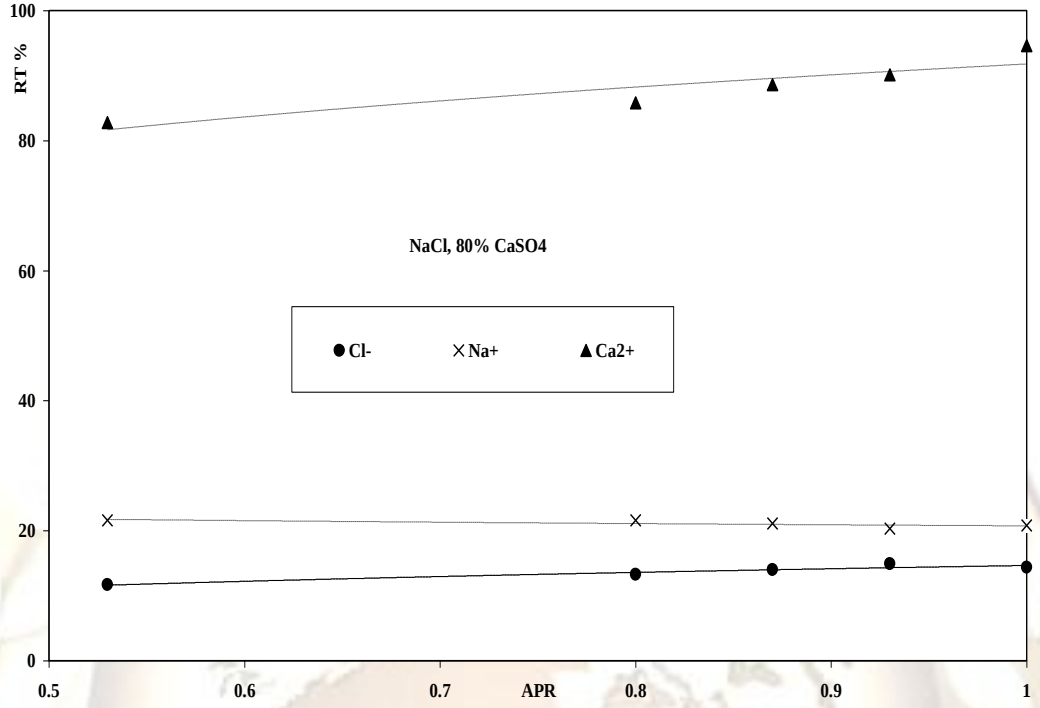

Figure 4: RO retention vs. applied reduced pressure.

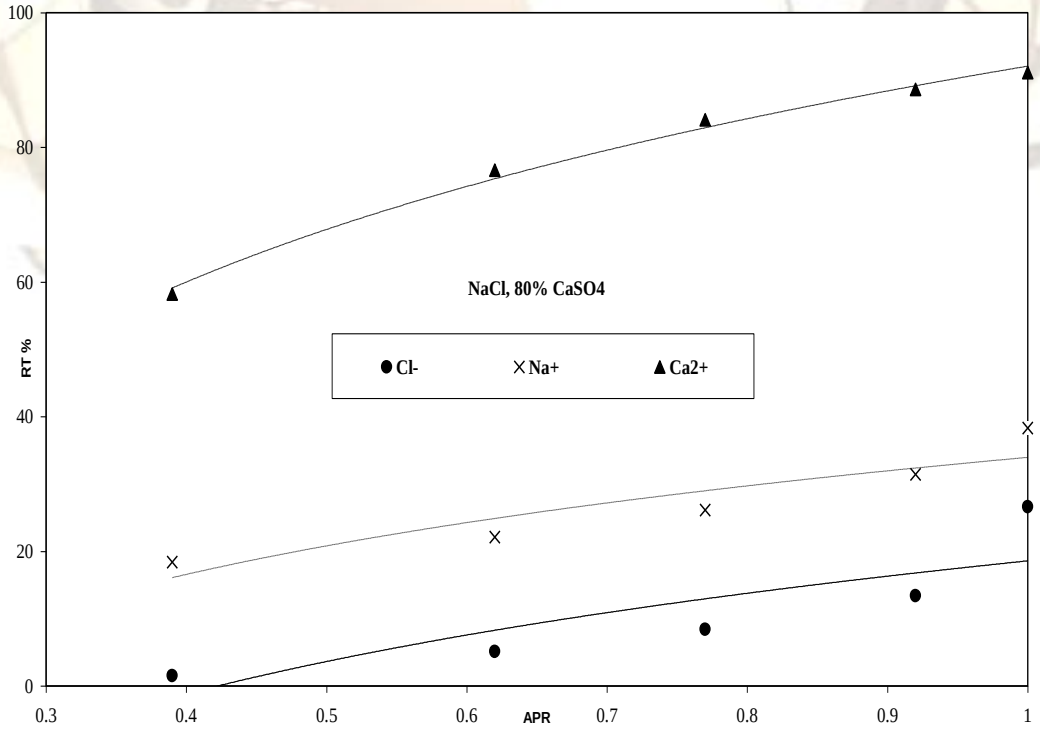

Figure 5: NF retention vs. applied reduced pressure.

On the other hand, employing solutions with low $CaSO_4$ mass fractions had caused the selectivity for both RO and NF membranes to be inverted as shown in Fig. 6 and 7 respectively. Here they reject more of the mono valent ions than that of the divalent ones. Such observation, that the divalent ions are rejected less than the mono-valent ions could seem to be contradicting with the more common view, that low pressure RO and NF membranes reject divalent cations very well [22].

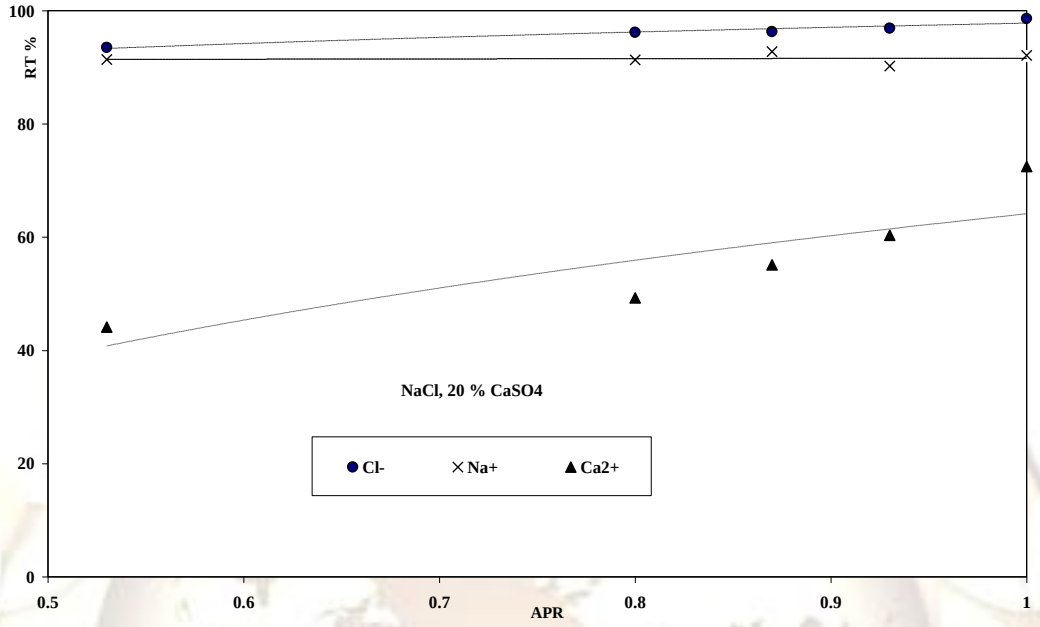

Figure 6: RO retention vs. applied reduced pressure.

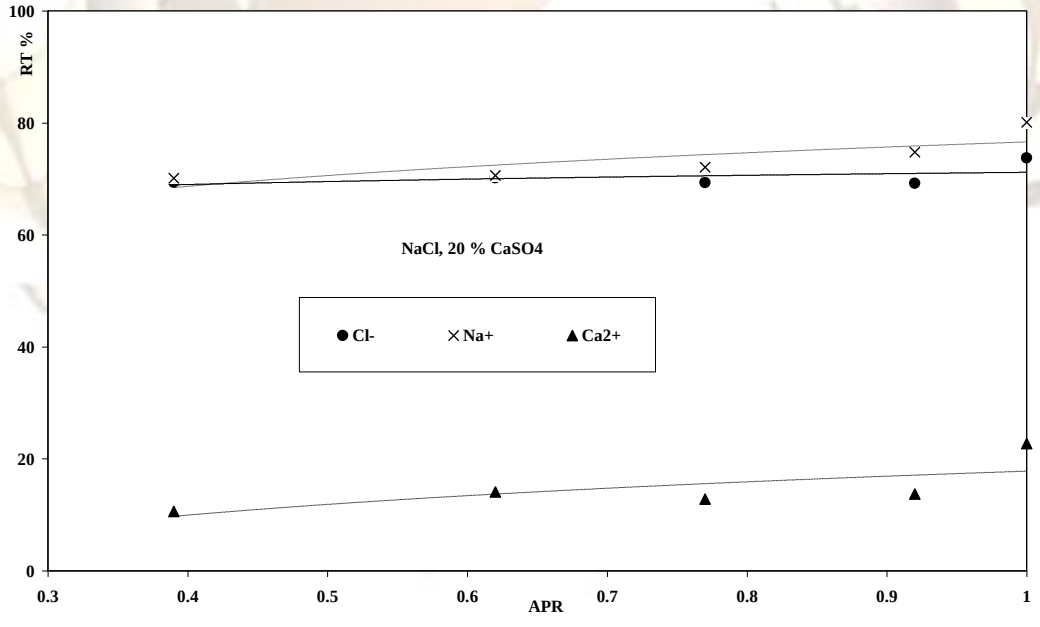

Figure 7: NF retention vs. applied reduced pressure.

Her et al. [23] and Cho et al. [24] have confirmed the negative charge of the NF 200, which was measured by the zeta potential measurements. In addition, Bellona and Drewes [25] have obtained by electrophoretic mobility and streaming potential measurements a negative potential zeta for the NF membrane. G. T. Ballet et al. [26] showed that for a negative charge of NF membrane, the retention for the divalent anion ($SO4^{2-}$) is the highest, whereas that of divalent cation (Ca^{2+}) is the lowest. The obtained RT is in agreement with Donnan exclusion

model. This model states that for a negatively charged membrane the increase in the co-ion charge and the decrease in the counter ion charge, would lead to an increase the RT of the salt. More over, the retention is not in accord with the size of the hydrated ions [27]. Therefore, the charge exclusion is the predominant mechanism for the salt removal by the NF 200 membrane.

Figure 8 represents the RT of Na^+ and Cl^- by the RO against the ARP for different $CaSO_4$ mass fractions in the solution. For the high mass fraction of $CaSO_4$, it is noticed that the RO membrane affinity to the Na^+ ion, is slightly higher than that to the Cl^- ions. This trend is inverted with the low mass fraction (20 %) of $CaSO_4$. The divalent calcium and magnesium are retained, while mono valent ions such as sodium and potassium are permeated through the membrane in order to maintain the electro-neutrality. The NF retention mechanism depends on the ion charge and the steric effects that take place across the membrane thickness [28]. The ARP has an insignificant effect on the retention.

Figure 9 shows the retention of the NF membrane for Na^+ and Cl^- ions against the ARP for different mass fractions for the $CaSO_4$ in the solution. This is noticeable that the NF membrane exhibits an affinity for the Na^+ cations slightly higher than that for the Cl^- anions. The ARP has insignificant effect on the retention of the membrane. These results are in agreement with the findings obtained in the case of the RO membrane.

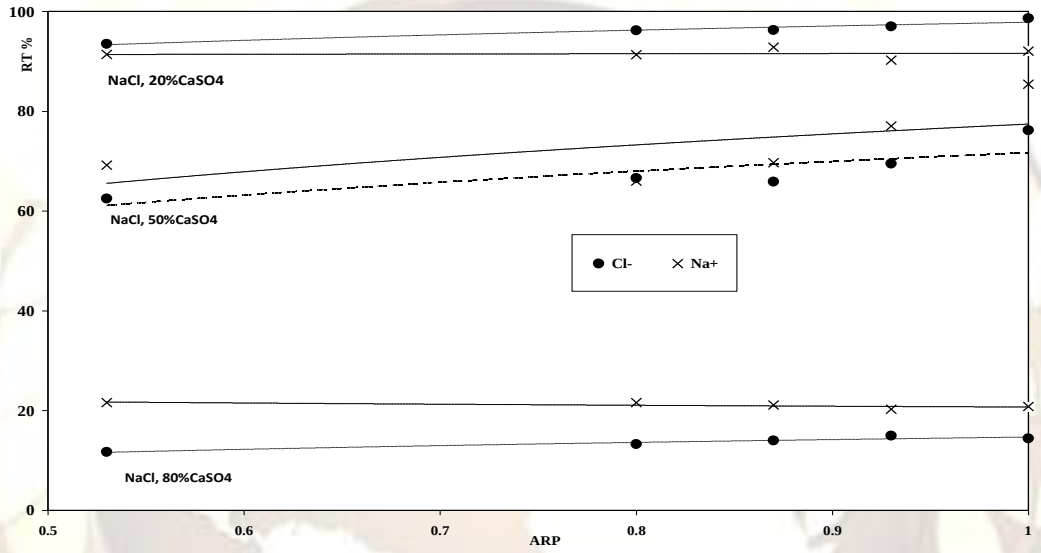

Figure 8: RO retention for Na^+ and Cl^- vs. ARP.

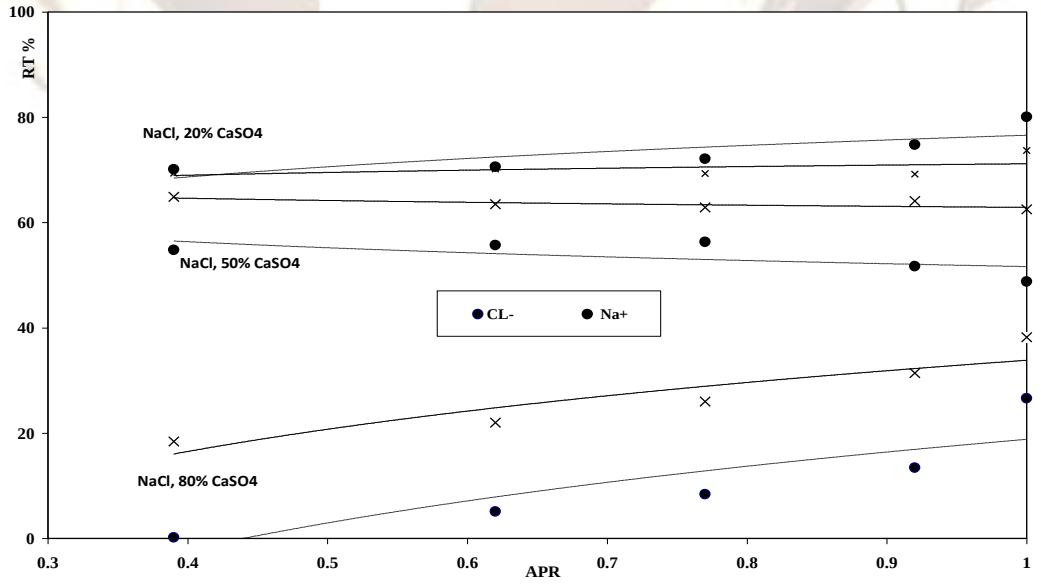

Figure 9: NF retention for Na^+ and Cl^- vs. ARP.

3.2. Evaluation of the integrated RO and NF modules

This part of the tests is focused on evaluating the performance of the integrated RO module and the NF module together either in series or in parallel configuration as shown in Fig. 10 and 11**.** Throughout these tests, the temperature and the feed water concentration are maintained at 20° C and 3.9 g/L respectively.

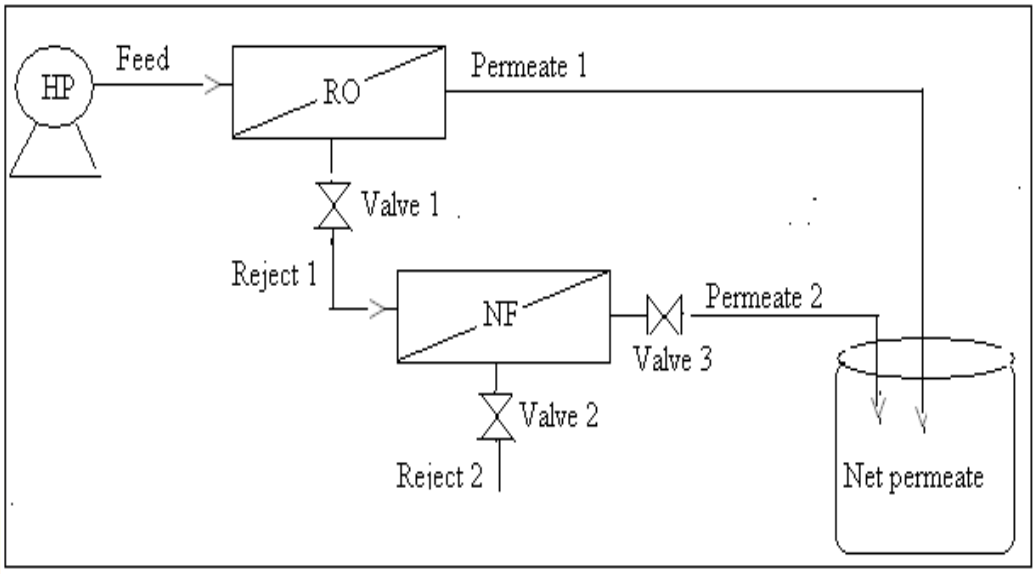

Figure 10: Series configuration for the setup.

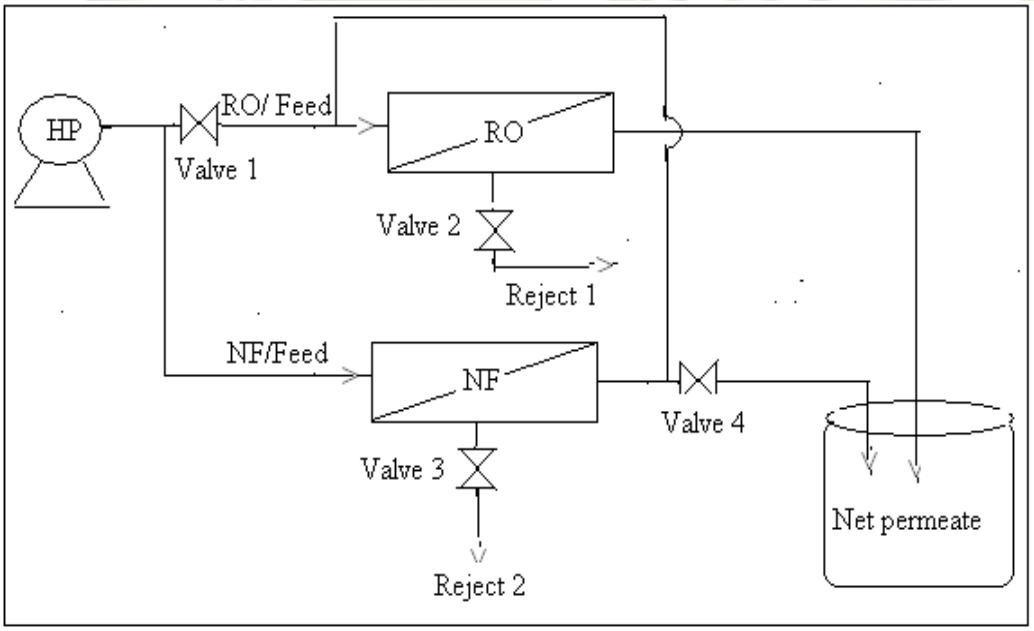

Figure 11: Parallel configuration for the setup.

3.2.1 - Flux characteristics for the integrated RO/NF setup:

Figure 12 shows the variation of the total flux produced by both, the RO and NF modules in series, and in parallel configurations as function of the ARP. The permeate flux is has a linear relationship with the applied pressure for both, series and parallel configurations. For the series configuration, the flux exhibits a substantial improvement, (4.4) about times that for the RO module (C_2: NaCl). Moreover, the quality of the permeate is better than that produced by the NF module. For the parallel configuration, however, the flux is slightly higher than that for the RO module.

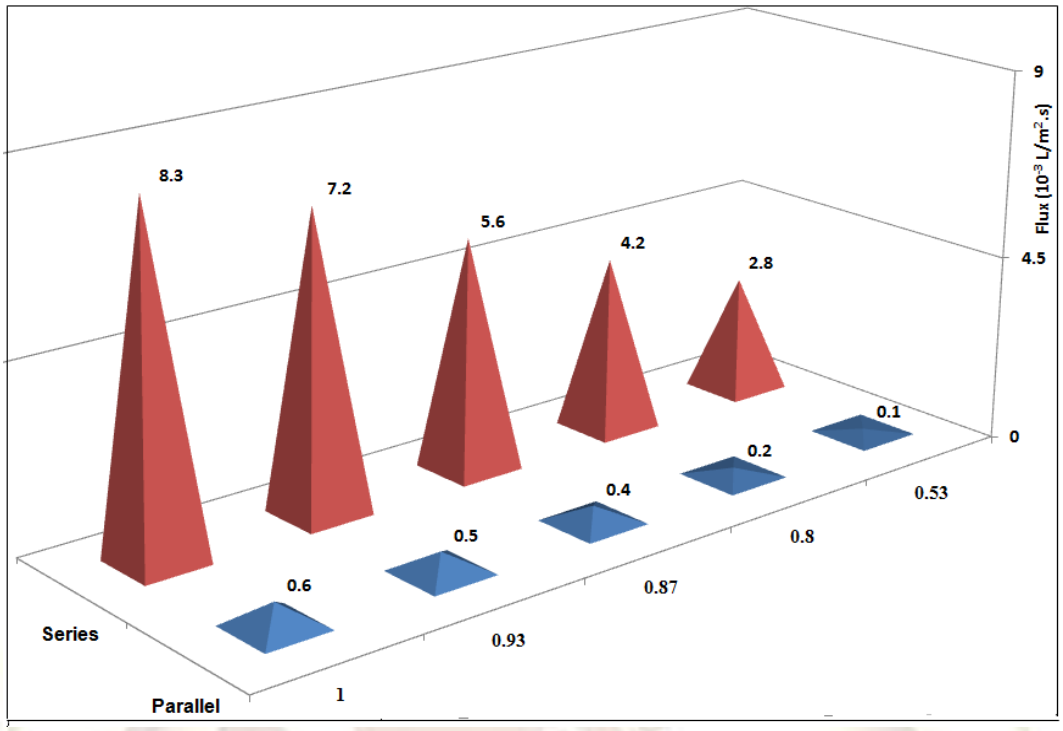

Figure 12: Flux vs. applied reduced pressure.

3.2.2 - Recovery ratio for the integrated RO/NF setup

The relation between the RR and the ARP, for the series and parallel configurations is shown in Fig. 13. It is noticeable that the RR increases by increasing the ARP for both the series as well as the parallel configurations. The RR exceeds 84.5 % at ARP = 1. This value is significantly higher than those obtained for the RO membrane (C_2: NaCl).

When the modules are set in the parallel arrangement, the RR varies from 5.6 % to 30.8 % when the ARP varied from 0.53 to 1 respectively. The increase in the RR is due to the decrease of the osmotic pressure at the entrance of the RO module. In that case, recycling the NF's permeate to the upstream of the RO module reduced the concentration of the feed going into the module.

3.2.3 - Retention for the integrated RO/NF setup

Figure 14 presents the relation between the RT and the ARP, for the integrated RO and NF modules, in both series and parallel arrangement. It shows that the RT increases gradually by increasing the ARP, and then it reaches an asymptotic value of about 43.5% and 83.2% for the series and the parallel configurations respectively.

For the series configuration, the RT is slightly higher than that of the single RO module (C_2: NaCl). However, in the parallel arrangement, the RT is substantially high compared with a RT of 8.3 % for the NF single module (C_2: NaCl).

3.2.4 - SEC for the integrated RO/NF setup

The relationship between the SEC in relation and the ARP for the cases of series and parallel configurations is as shown in Fig.15. In general, there is a substantial reduction in the SEC with increasing the value of the ARP for both cases to the pressure for series as well as for parallel.

When the modules are arranged in series, the value for the SEC reaches a minimum of 7.9 kJ.L^{-1} at an ARP = 1. It is worth mentioning that at an ARP =1, the SEC of the RO module alone was 42.35 kJ.L^{-1} for the feed concentration of C_2 (NaCl). Figure15 also shows that the SEC for the parallel arrangement, on average, is about twenty times that for the series arrangement.

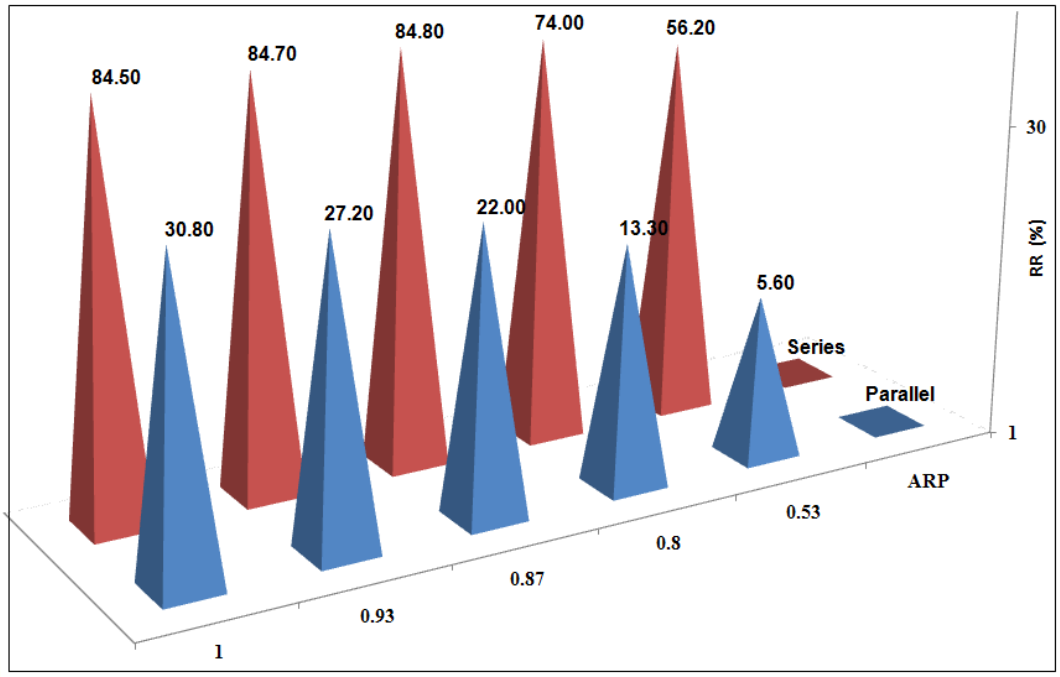

Figure 13: RR % vs. applied reduced pressure.

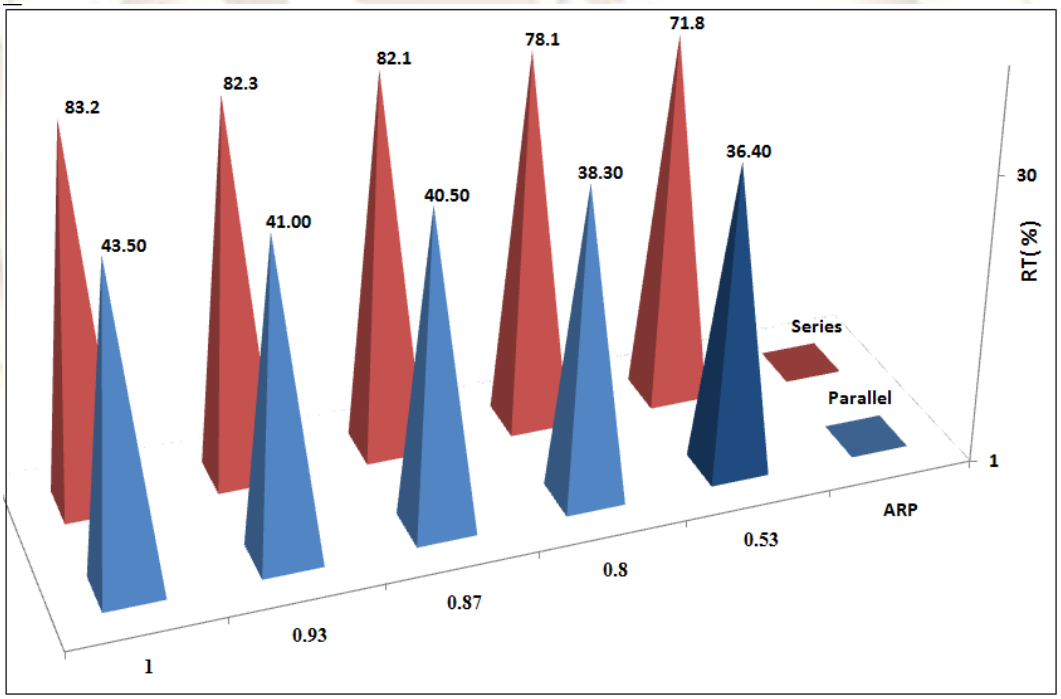

Figure 14: Retention vs. applied reduced pressure.

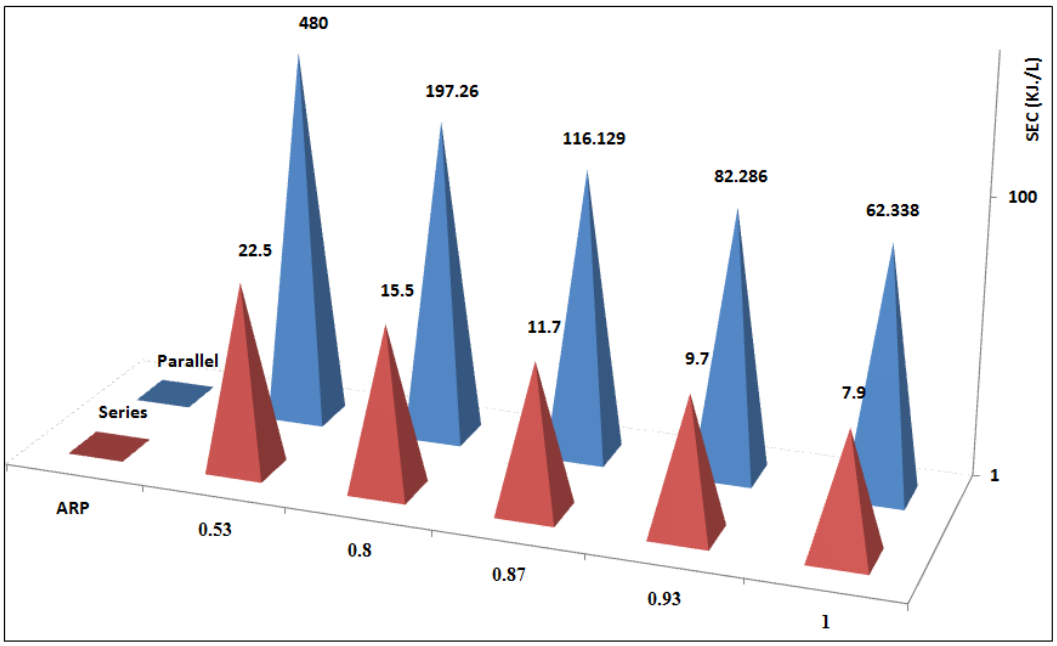

Figure 15: SEC vs. applied reduced pressure.

3.2.5 - Selectivity for the integrated RO/NF setup

Figures 16 and 17 show the variation in the retention of the cations Na^+, K^+, Ca^{2+} and Mg^{2+}, for the parallel and series arrangements respectively. The following observations could be made:

a) The retention of the parallel configuration for single valence ions varies from 87 % for Na^+ to 96 % for K^+, which is higher than that obtained using the series configuration with 8 % for Na^+ and 19.6 % for K^+.

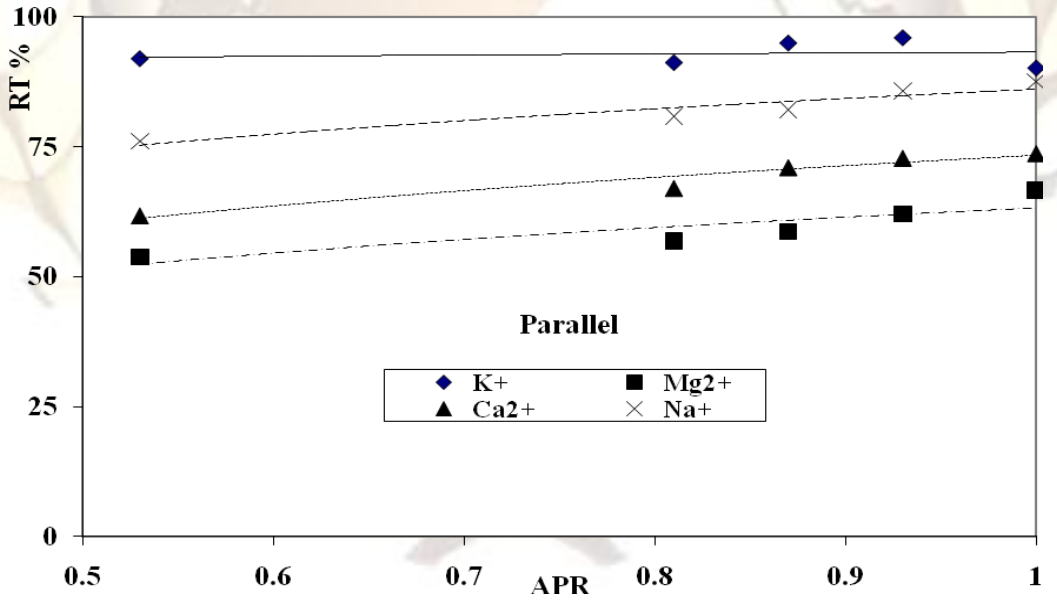

Figure 16: Retention of cations vs. applied reduced pressure.

b) The selectivity of the divalent ions, e.g. Ca^{2+} and Mg^{2+} in the parallel assembly is 73 % and 66 %, compared with 61.8 % and 53.3 % for the series assembly respectively. Such results indicate that the parallel configuration would present low s risk of scaling for the RO membrane.

c) The parallel assembly would produce permeate with higher quality compared with that obtained from the series assembly.

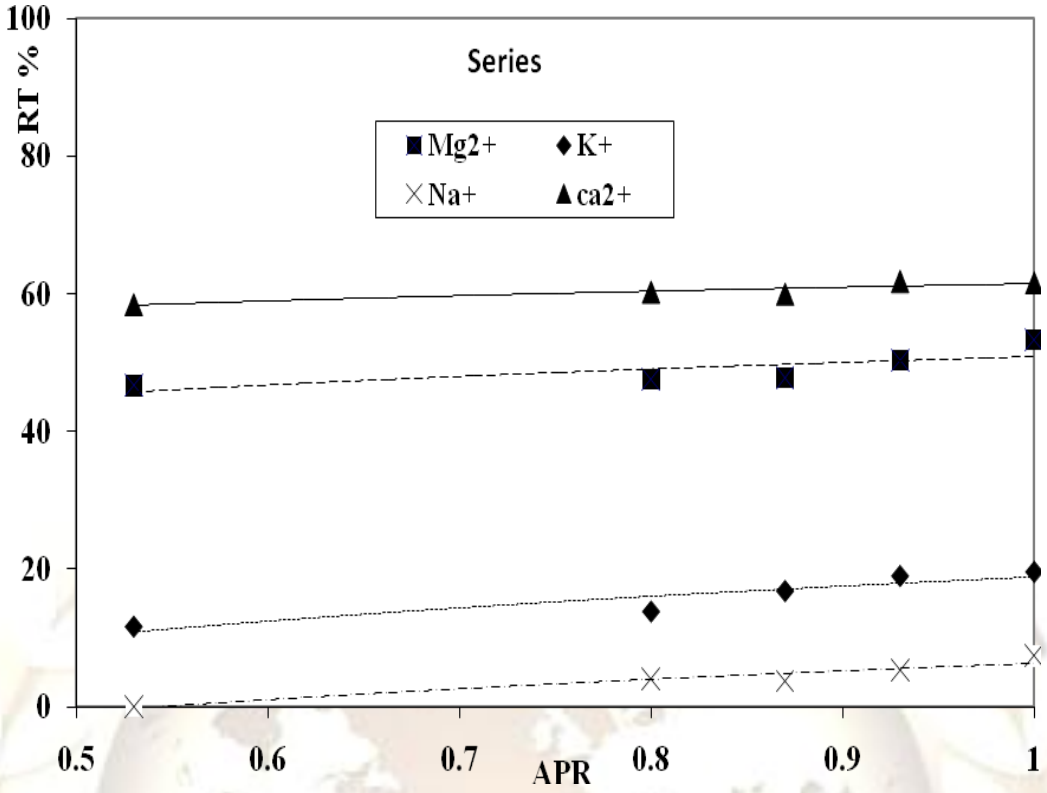

Figure 17: Retention of cations vs. applied reduced pressure.

3.3. Integrated setup characteristics at ARP = 1

Since membrane desalination plants are usually operated at the design conditions ,i.e. at ARP of unity, thus studying the present integrated setup at ARP of unity worth's being focused at. Figures 18 and 19 show the performance of the integrated RO / NF setup in both series and parallel configurations at APR = 1, and at a feed water concentration of 3.9 g/L , under constant temperature of 20°C. The results for that case study are summarized as following:

3.3.1 Flux characteristics for the setup at ARP= 1

The data given in Fig. 18 show that, the permeate flux for the series configuration is 6 times that of the RO module (C_2: NaCl), with a permeate quality higher than that of the NF module. The RR% exceeds 30.8 % and it is widely superior to those obtained in RO membrane (C_2: NaCl). The RT reaches an asymptotic value of 43.5 %. The SEC in this configuration is 7.9 $kJ.L^{-1}$, compared with 42.35 $kJ.L^{-1}$ for the RO at feed concentration C_2 (NaCl).

As far as the performance of the parallel configuration is concerned, Fig.18 shows that, the flux is slightly higher than that of the RO module; however, it is 13.8 times that for the series configuration. The RR of the parallel configuration reaches 84.5 %, 3 times that for the series configuration, due to the decrease in the osmotic pressure at the entrance of the RO module in the assembly. Indeed, recycling of the NF permeate to the upstream of the RO module had improved the assembly characteristics. The SEC for the series configuration is about 8 times that for the parallel configuration.

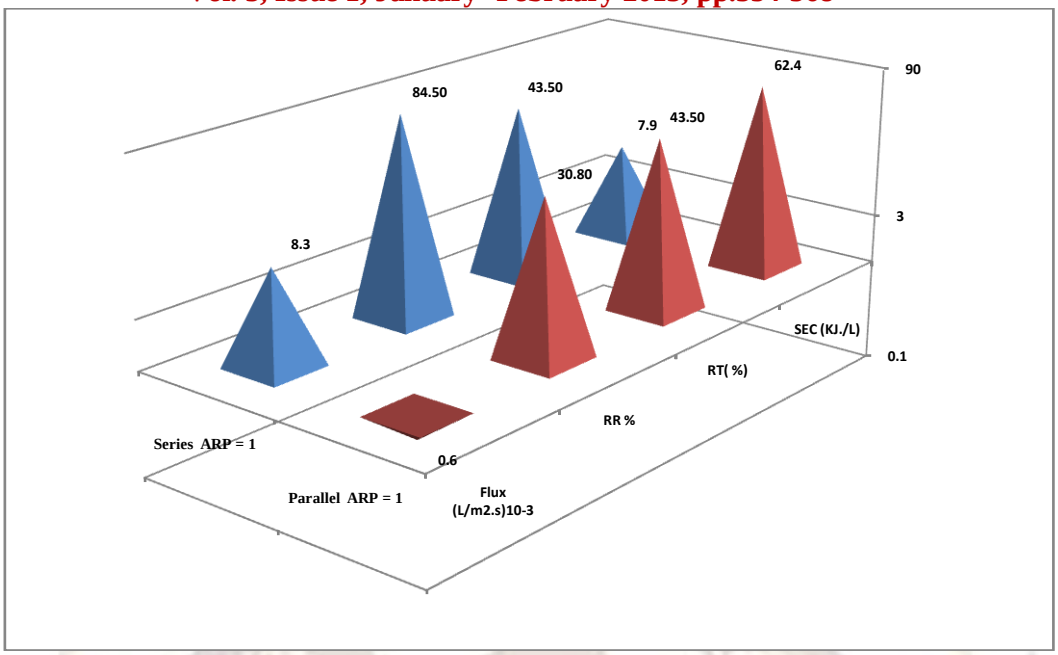

Figure 18: Performance of integrated RO and NF modules in series and parallel configuration.

3.3. 2 - Selectivity for the setup at ARP = 1

Figure 19 shows the RT% of the cations for both parallel and series configurations. It is clear that, the parallel configuration is more capable of cations retention than the series configuration. This is attributed to the favorable effect of the NF permeate recycling of on the characteristics of the RO module, and thus the permeate quality for the parallel configuration should be equal or more than that of the RO module. Such advantage for the parallel configuration is inverted in term of the total flux.

It is worth mentioning that, the series configuration is more capable for retaining the divalent cations more than the mono valent cations. Such trend, as shown in Fig. 19, is opposite to that for the parallel configuration.

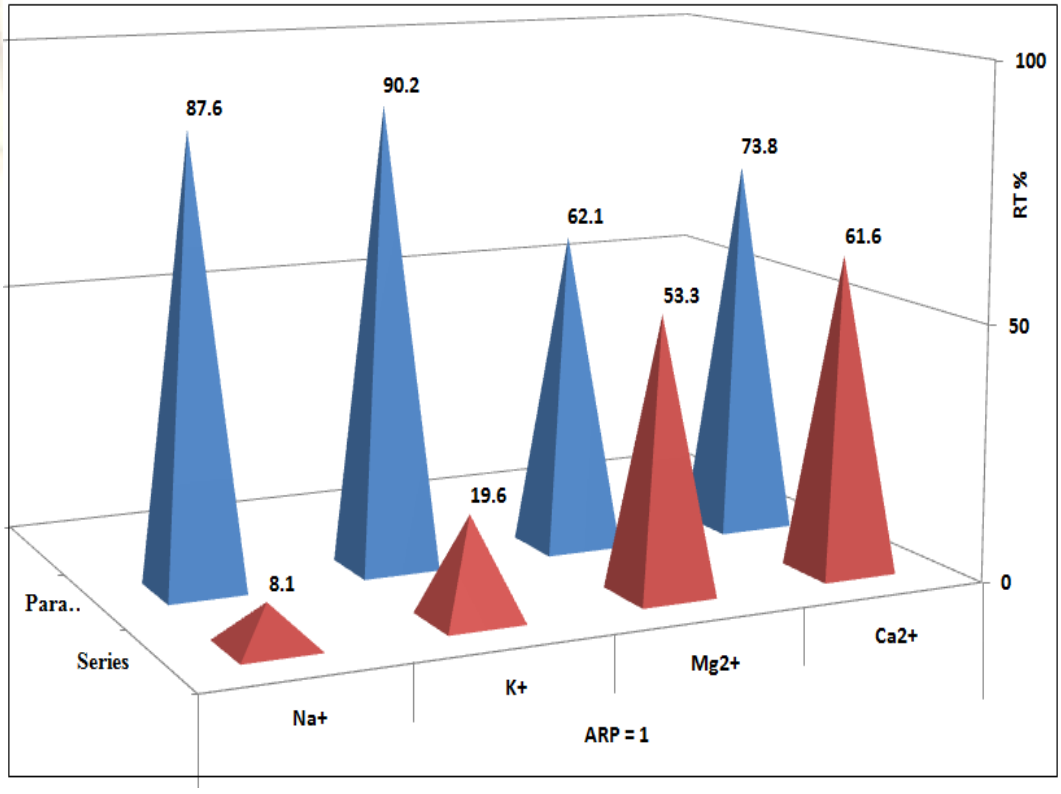

Figure 19: Retention of cations in series and parallel configurations.

4. Conclusion

The present work was initiated by a desire to, (A) Compare the performance of one RO module and one NF module separately, one at a time, and (B) Study the performance of an integrated membrane setup for a desalination test pilot plant. A setup is made that comprises one RO module and one NF module are integrated, and powered by photovoltaic panels. The conclusions from (A) and (B) could be summarized as following:

Characteristics of the RO and NF membranes show their potential regarding their permeability and capabilities for retaining the solute components from the feed. The RO membrane distinguishes itself by a higher retention of the ions (mono and divalent ions) than the NF membrane. The RO membrane retention for the divalent ions is higher than that for the single valent ions. The NF membrane is more permeable than the RO membrane.

The flux from the NF module is significantly higher than that of the RO, and the SEC for the NF module is much lower than that for the RO module.

The integrated RO/NF modules, in series and parallel configurations, offer an alternative to operate the membrane desalination test plant according to the nature of the compulsory constraint. It provides an opportunity to maximize the benefits from both membranes, which will contribute in reducing the cost of the fresh water produced.

For well-balanced feed water with a moderate level of salinity, e.g. water softening, the series assembly could ensure a high water recovery ratio at a reduced SEC. That will considerably reduce the required PV panels. However, for a feed with high solute concentration, the parallel assembly presents a reasonable solution to operate the membrane desalination system at less risk of scaling for the RO membrane.

References

[1] A. Ghermandi, R.Messalem, Solar-driven desalination with reverse osmosis: the state of the art, Desalination and Water Treatment, 7 (2009) 285–296.

[2] C. Fritzmann, J. Loewenberg, T. Wintgens and T. Melin, State-of-the-art of reverse osmosis desalination. Desalination, 216 (2007) 1–76.

[3] M. Wilf, Fundamentals of RO–NF technology, Proc. International Conference on Desalination Costing, Middle East Desalination Research Center, Limassol, Cyprus, 2004.

[4] M. Wilf and K. Klinko, Optimization of seawater RO systems design. Desalination, 138 (2001) 299–306.

[5] S. Alawaji, M.S. Smiai, S. Rafique and B. Stafford, PV-powered water pumping and desalination plant for remote areas in Saudi Arabia. Appl. Applied Energy 52 (1995) 283 –28**9**.

[6] S. Abdallah, M. Abu-Hilal and M.S. Mohsen, Performance of a photovoltaic powered reverse osmosis system under local climatic conditions. Desalination, 183 (2005) 95–104.

[7] D.G. Harrison, G.E. Ho and K. Mathew, Desalination using renewable energy in Australia. Renewable Energy, 8 (1996) 509–513.

[8] Tripanagnostopoulos, Th. Nousia, M. Souliotis, and P. Yianoulis (2002), Hybrid Photovoltaic/Thermal Solar Systems, *Solar Energy* Vol. 72, No. 3, pp. 217–234.

[9] B.S. Richards, D.P.S. Capão and A.I. Schäfer, Renewable energy powered membrane technology. 2. The effect of energy fluctuations on performance of a photovoltaic hybrid membrane system. Environ. Sci. Technol., 42(12) (2008) 4563–4569.

[10] S. Bouguecha, B. Hamrouni and M. Dhahbi, Small scale desalination pilots powered by renewable energy sources: case studies. Desalination, 183 (2005) 151–165.

[11] A. Hassan, M. A1-So, A. A1-Amoudi, A. Jamaluddin, A. Farooque, A. Rowaili, A. Dalvi, N. Kither, G. Mustafa and I. AI-Tisan, A new approach to thermal seawater desalination processes using nanofiltration membranes (Part 1), Desalination, 118 (1998) 35-51.

[12] M. A1-Sofi, A. Hassan, G. Mustafa, A. Dalvi and M. Kither, Nanofilltration as a means of achieving higher TBT of ~ 120 degrees C in MSF, Desalination, 118 (1998) 123-129.

[13] M. A1-Sofi, Seawater desalination– SWCC experience and vision, Desalination, 135 (2001) 121-139.

[14] E. Dlioli, F. Laganh, A. Crlscuoh and G. Barbieri, Integrated membrane operations in desalination processes, Desalination, 122 (1999) 141-145.

[15] H. Ohya, T. Suzuki and S. Nakao, Integrated system for complete usage of components in seawater: A proposal of inorganic chemical combination seawater, Desalination, 134 (2001) 29-36.

[16] E. Drioli, A. Criscuoli and E. Curcioa, Integrated membrane operations for seawater desalination, Desalination, 147 (2002) 77-81.

[17] Andrea I. Schäfer and Bryce S. Richards, Testing of a hybrid membrane system for groundwater desalination in an Australian

national park, Desalination, 183 (2005) 55-62.

[18] Andrea Ghermandi, Rami Messalem , The advantages of NF desalination of brackish water for sustainable irrigation: The case of the Arava Valley in Israel, Desalination and Water Treatment, 10 (2009) 101–107.

[19] H.M. Krieg , S.J. Modise b, K. Keizer ¢, H.W.J.P. Neomagus Salt rejection in nanofiltration for single and binary salt mixtures in view of sulfate removal, Desalination 171 (2004) 205-215.

[20] GM. Rios and R. Joulie, Investigation of ion separation by microporous nanofiltration membranes. AIChE J., 42 (9) (1996) 2521-2528.

[21] Colon W. "Pilot field test data for prototype ultra low pressure reverse osmosis element," Desalination, 56 (1985) 203–226.

[22] A. K. ZANDER and N. K. CURRY, Membrane and solution effects on solute reject and productivity, Water Research. 35 (18) (2001) 4426–4434.

[23] N. Her, G. Amy, C. Jarusutthirak, Seasonal variations of nanofiltration foulants: identification and control, Desalination 132 (2000) 143–160.

[24] Cho, J., Amy, G., Pellegrino, J., Membrane filtration of natural organic matter: initial comparison of rejection and flux decline characteristics with ultrafiltration and nanofiltration membranes. Water Res. (1999) 2517-2526.

[25] C. Bellona, J.E. Drewes, The role of membrane surface charge and solute physico-chemical properties in the rejection of organic acids by NF membranes, J. Membr. Sci. 249 (2005) 227–234.

[26] G. T. Ballet, A. Hafiane, M. Dhahbi, Influence of operating conditions on the retention of phosphate in water by nanofiltration, Journal of Membrane Science 290 (2007) 164–172.

[27] M.Y. Kiriukhin, K.D. Collins, Dynamic hydration numbers for biologically important ions, Biophys. Chem. 99 (2002) 155–168.

[28] Courfia K. Diawara, Nanofiltration Process Efficiency in Water Desalination, Separation & Purification Reviews, 37 (3) (2008) 302-324.